

ARTICLE

Flexibility in MOFs: do scalar and group-theoretical counting rules work?

Cite this: DOI: 10.1039/x0xx00000x

A. Marmier^{a‡} and K.E. Evans^a

Received 00th January 2015,

Accepted 00th January 2015

DOI: 10.1039/x0xx00000x

www.rsc.org/Dalton

We investigate the ability of counting rules drafted from engineering to predict the flexibility or rigidity of bar-and-joint or body-and-joint assemblies representing metal organic frameworks. We show that while scalar counting rules are not reliable, group-theoretical approaches are able to disentangle mechanisms from states of self-stress and to predict the existence of flexible mechanisms. We give several detailed examples of such calculations, highlighting the fact that behind an abstract exterior they are in fact easy to apply and similar to the method used to obtain molecular vibrations. We also correct a slight misinterpretation of the rigidity of IRMOF-1.

1 Introduction

The concept of flexibility, when associated with hybrid frameworks, remains ill-defined and often means different things to different researchers. In this study we focus on the flexibility of underlying frameworks composed of mechanical objects such as bodies, bars and joints, representing the linkers and Secondary Building Units (SBUs) of a hybrid crystal. Our main aim consists in applying several flavours of counting rules, from simple (but subtle) scalar versions to powerful group-theoretical formulations in order to determine whether they can reliably be applied to determine flexibility. Using counter-examples, we prove that the simpler scalar counting rules do not work for 3 dimensional (3D) metal organic frameworks (MOFs) because the underlying frameworks are highly over-constrained and the number of states of self-stress conceals the number of mechanism. On the other hand, we apply symmetry extended versions of the counting rules to two MOFs (IRMOF-1 –MOF5– known to be rigid, the other a body centred cubic net known to be flexible) and show that this method can correctly predict flexibility and rigidity for MOFs.

Whether a MOF is rigid or flexible is important for several applications. In some cases, for instance in order to control the release of bio-active drugs¹, flexibility is essential to tailor diffusion. In other cases, for instance gas storage² or capture³, flexible materials with associated low stiffness will undergo cyclical load/unload strains and are likely to fail by fatigue mechanisms.

The next section discusses several concepts of flexibility, and some elements of reticular chemistry. Section 3 introduces the formalism for flexibility of frameworks, starting with the simpler scalar counting rules, and incorporating several subtle

aspects that we have not seen in prior works. In this section, we also consider periodic extensions to the scalar counting rules, introduce two test cases and conclude that scalar counting rules are not applicable. In section 4, we describe the basics of the symmetry extended extensions of the counting rules, and show that they correctly predict the flexibility or rigidity of the two test cases. We conclude that the method is simple to apply and adapted to the variety of MOFs, and propose developments.

2 Background

2.1 Flexibility of crystals and organic frameworks

The study of the rigidity/flexibility (often mobility in the mechanical/machine literature) of structures is of interest in several disciplines: mathematics⁴⁻⁶, engineering^{7, 8}, chemistry⁹⁻¹¹. In this context, some of the literature can be somewhat difficult to approach for practitioners of a different discipline and the language used to describe similar concept can be inconsistent. Table 1 provides a non-exhaustive list of relevant keywords. Several engineering terms need clarifying. In this study, a MOF is modelled as a structure composed of rigid bodies (ligands and possibly SBUs) connected by mechanical joints. These joints can be of several types but only three seem relevant to MOFs. A fixed joint does not allow any degree of freedom. A so-called spherical joint (also ball, or spheroidal) would allow three degrees of freedom, three rotations. An especially important joint for carboxylate ligand MOFs is the hinge joint (also knee-cap or pin-joint or revolute) that only allows one degree of freedom, a rotation. Depending on the way the bodies are assembled, the structure can be rigid or flexible. If it is flexible, it can deform and the modes of

deformation are called mechanisms. A mechanism also corresponds to a degree of freedom of the structure. In flexibility theory, mechanisms are the analogues of normal modes in vibration theory. If the structure is rigid, it can either be just rigid, which corresponds to having exactly 0 degrees of freedom, or it can be over-constrained. In a just rigid structure, slightly inexact dimensions (for instance poor tolerances or thermal expansion) can be readily accommodated. In an over-constrained structure, additional bodies are in a so-called state of self-stress because any small deviation from the exact geometry would result in distortions in several bodies. In fact, over-constrained structures cannot be solved by considering the equations of static equilibrium only, and so-called constitutive equations taking into account the elasticity of bodies must be included: these problems are often called “statically indeterminate”. The first three structures in table 2 illustrate the concepts of flexibility, rigidity and over-constraining. Note also that a structure can contain both mechanisms and states of self-stress, as shown by the fifth structure in table 2.

Early engineers and architects must have had an intuitive understanding of the rigidity of structures for a long time, and a formal rigidity theory only starts in the second half of the nineteenth century. Gogu's review⁸ provides an interesting historical section that shows the contribution of the pioneers and references to early works. In engineering, the determination of the degrees of freedoms (DOFs) of a machine is important and still very relevant today, from the simple linkages undergraduate start with, to complex kinematic chains relevant to robotic motion¹².

Table 1. Terminologies relevant to MOF flexibility

Organic Framework	Secondary Building Block, Clusters	Ligand, Linker
Net	Vertices	Links
Graph	Node	Edge
Framework, Truss, Structure, Skeletal Structure	Joint	Bar, Two-force member
Mechanism, Machine, Kinematic Chain, Assembly	Joint	Body, Linkage

In a chemical context, an interest in the flexibility of crystals perhaps starts with Pauling's study of sodalite¹³. In fact, much of the chemical thinking on rigidity derives from the study of zeolites. A first class of approaches consists in exploring the phonon spectrum of zeolites and identifying vibration modes that conserve the shape and size of tetrahedra and have low frequency; these modes are variously referred to as rigid unit modes¹⁴ (RUM) or floppy modes¹⁵ depending on the implementation. More recently⁹, the concept of a flexibility window has emerged, where many zeolites remain flexible in a range of density; it is postulated that zeolites with a large flexibility window are more realisable^{16, 17}.

In a few rare studies, rigid-units^{18, 19} and flexibility windows²⁰ type approaches have been applied to MOF-like structures. Other ideas have also been tried. In a review on “breathing” MOFs²¹, Ferey and Serre propose a list of empirical rules based on symmetry of the SBU. In a series of *ab initio* simulation

studies, Coudert²²⁻²⁴ and co-workers have shown that there is a strong correlation between flexibility and large elastic anisotropy: this is explained by the fact that if a mechanism exists, then distortions in the direction that activate it will necessarily be very soft with a correspondingly very low modulus (Young's or shear), and therefore the ratio of maximum modulus by minimum modulus must be high (they propose 20 as an arbitrary cut-off).

Another numerical approach¹⁰ for MOFs has recently been proposed by Sarkisov and co-workers. It is based on mapping MOFs to equivalent molecular truss systems and perturbing the unit cells for different distortions. The analysis is then comparable to atomistic force field simulations as the molecular trusses are modelled as stiff harmonic springs, and the total energy is minimised for each deformation. A rigid framework is one which experiences high energy penalty for all deformations, while a flexible framework has a very low penalty for at least one deformation mode. This technique is somewhat related to the RUM approach through the use of artificial springs. It also highlights the same tendency in chemistry to formulate problems that can be solved by tools such as energy optimisation and lattice dynamics for which algorithms are widely known and often already implemented in libraries and packages.

On the mechanical side, approaches to solving the mobility problem have chiefly been based on setting up a kinematic (compatibility) matrix and solving the corresponding eigenvalue problem to obtain the null-space (see for instance^{25, 26}, and^{16, 27} for an application to zeolites). These approaches are perhaps more rigorous than those based on energy optimisation of systems of “springs”, but algorithms and implementations have been less accessible, probably for historical reasons.

Finally, Guest and Fowler have been developing procedures based on group theory that have been applied with success to mechanical^{28, 29} and chemical^{30, 31} problems. The main advantages of these schemes are that they simple enough to be performed “by hand”, and general enough to include all sort of joints and be extended to periodic³¹ systems.

2.2 MOFs as frameworks

Any molecule or more generally any chemical object can be mapped onto several graphs, where at the simplest level the atoms could be the nodes and the bonds could be the edges (other, coarser grained mapping are possible, and in the case of MOFs desirable). This is the main principle behind the concept of reticular chemistry of Yagi and O'Keefe³², which was developed to provide a nomenclature for the ever expanding MOFs and more generally hybrids systems. The Reticular Chemistry Structure Resource provides a database to identify and possibly design new materials. At its core is the concept of periodic nets, which can be represented by a code based on a three letter symbol.

3 Scalar counting rules

3.1 Basic Maxwell-Caladine criteria

The basic counting rules were established by Maxwell³³ and clarified by Calladine⁷. They can be applied to a framework containing b bars linked by j joints (always revolute (“pin”) in 2D, always spherical in 3D). The difference between the number of mechanism m and the number of self-stresses s is given by equation (1) in 2D and equation (2) in 3D,

$$(2D) \quad m - s = 2j - b - 3, \quad (1)$$

$$(3D) \quad m - s = 3j - b - 6. \quad (2)$$

These formulations emphasise the joints and can be derived by considering a system of j points in a space of dimension d . Each point brings d DOFs (translations), each bar/bond introduces one constraint and removes one DOF (in any dimension), and some DOFs are trivial translations or rotations and must be removed (3 in 2D, 6 in 3D). This procedure is familiar as it is very similar to the one used to calculate the number of vibration modes in a molecule.

The central limitation of all counting rules is already in evidence here: they do not provide directly the mobility or number of DOF of a mechanism, but subtract the number of states of self-stress. As a consequence, in an over-constrained system, mechanisms can be hidden by states of self-stress.

Looking forward towards our main aim of predicting flexibility in MOFs, another obvious shortcoming of the Maxwell rule in 3D is that it can only handle spherical joints. That is likely to be too limiting where the SBU-ligand connection is more restrictive, and behave more like a hinge, as is common for carboxylate linkers for instance.

3.2 Basic Chebychev–Grübler–Kutzbach criteria

Fortunately, other formulations exist, which this time focus on bodies (sometimes called linkages), more complex than bars, that are linked by joints of different types. These formulations were derived independently by Chebychev³⁴, Grübler³⁵ and Kutzbach³⁶, and will therefore be referred to as CGK criteria or counting rules (many more formulae exists, as listed in⁸, but they derive from these early works). They are used extensively in machine design and kinematic theory in order to determine the DOFs of a machine/mechanism. Considering an assembly of n bodies linked by g joints, each of which possesses f_i DOFs, the difference between the number of mechanism m and the number of self-stresses s is given by

$$(2D) \quad m - s = 3(n - 1) - 3g + \sum_{i=1}^g f_i, \quad (3)$$

$$(3D) \quad m - s = 6(n - 1) - 6g + \sum_{i=1}^g f_i. \quad (4)$$

The same remarks as for the Maxwell criteria concerning the relation between mechanism and states of self-stress apply, and in an over-constrained system, the later can hide the former.

Equations (3) and (4) give access to systems with richer joints than their Maxwell counterparts. In 2D, 3 types of joints exist: pin-joint (1 DOF, rotation), slider-joint (1 DOF, translation) and the pin slider joint (2 DOFs). In 3D, several complex joints can be created, with up to 3 DOFs in practice. Those relevant to

SBU-linker connections are spherical joints (3 DOFs, all rotations) and revolute joints, “hinges”, with 1 DOF, a rotation.

Table 2. Examples of counting rules for simple 2D frameworks

Framework	Maxwell $m - s = 2j - b - 3$	Naïve CGK $m - s = 3(n - 1) - 3g + \sum_{i=1}^g f_i$	Correct CGK $m - s = 3(n - 1) - 3g + \sum_{i=1}^g f_i$
	(4, 4) $\Rightarrow m - s = 1$	(4, 4, 4 × 1) $\Rightarrow m - s = 1$	(4, 4, 4 × 1) $\Rightarrow m - s = 1$
	(4, 5) $\Rightarrow m - s = 0$	(5, 4, 4 × 1) $\Rightarrow m - s = 4$	(5, 6, 6 × 1) $\Rightarrow m - s = 0$
	(4, 6) $\Rightarrow m - s = -1$	(6, 4, 4 × 1) $\Rightarrow m - s = 7$	(6, 8, 8 × 1) $\Rightarrow m - s = -1$
	(6, 9) $\Rightarrow m - s = 0$	(9, 6, 6 × 1) $\Rightarrow m - s = 12$	(9, 12, 12 × 1) $\Rightarrow m - s = 0$
	(6, 9) $\Rightarrow m - s = 0$	(9, 6, 6 × 1) $\Rightarrow m - s = 12$	(9, 12, 12 × 1) $\Rightarrow m - s = 0$
	N/A	(8, 8, 8 × 1) $\Rightarrow m - s = 5$	
	N/A	(9, 10, 10 × 1) $\Rightarrow m - s = 4$	
	N/A	(10, 12, 12 × 1) $\Rightarrow m - s = 3$	

Table 2 displays eight 2D frameworks and shows the corresponding results from different counting schemes.

The first three frameworks illustrate well the concept of self-stress: in the third framework, the last bar over-constrains the system, which is then statically indeterminate (from a mechanical perspective, this means that the equilibrium equations are not enough to determine the states of stress in each member).

These frameworks also demonstrate that the CGK rule must be applied with great care. The number of joints g in particular is not always obvious to determine. It is no accident that the number of “joints” in equations (1,2) and (3,4) are represented by different symbols (j and g respectively): they are different quantities. A naïve reading of equation (2) would conflate j and g , and leads to $f_M \neq f_{CGK}$. This is because the traditional representation superposes the joints, and conceals some of them, as shown in Fig. 1.

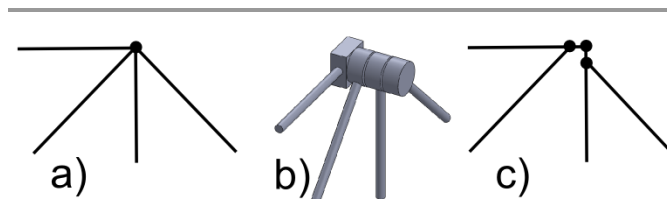


Fig. 1. (a) Simplified representation where four body-bars are connected by pin-joints, the correct number of joints is not immediately apparent, (b) Possible physical realisation, showing three pin-joints, (c) Topologically correct representation, with three pin-joints.

The fourth and fifth frameworks in table 2 show that with the exact same numbers of joints and bars, both structures are predicted to have the same number of mechanisms and states of self-stress. But it is only by inspection that we can see that the fourth structure has no mechanisms and no states of self-stress while the fifth structure has one of each. The usefulness of the counting rule is certainly reduced in that last case, as the state of self-stress conceals the mechanism.

In addition, the counting rules ignore the geometry of the system and only consider its broad topology. In machine design this leads to the well-known existence of extra “geometric” DOFs which are not predicted by the counting criteria, but which occur because some bodies are aligned in very specific ways (for instance parallel bars, see Fig. 2).

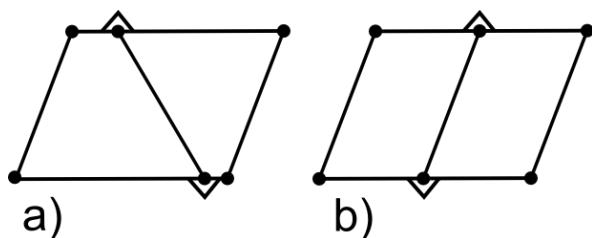
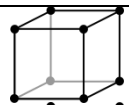
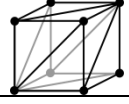


Fig. 2. 5-bars linkages (the triangular symbols are standard and indicate that the linked bars form single rigid bodies, without them the figures would represent 7-bars linkages), the CGK criterion predicts 0 DOFs. (a) Topologically general representation, where it is obvious the mechanism is locked. (b) Geometrically specific configuration, where one DOF emerges from parallel bars.

While chiefly intended to illustrate the existence of geometric DOFs, Fig. 2 also shows one of the limitations of the Maxwell counting rules: they are only applicable to systems where a joint is located at the end of bars, and cannot handle joints on the body of a bar. In the language of mechanics, only trusses composed of two-force members (bars) can be analysed by the Maxwell rules.

The CGK counting rules operate on more complex bodies and can be applied to systems such as in Fig. 2. We have already seen that part of the price to pay for this richness is that extra care must be taken to count the joints. An additional subtlety not apparent in 2D reveals itself in 3D: even if one wants to just use simple “bars”, in the CGK formalism these are actually complex objects with 6 DOFs (a bar has an axis of symmetry and only 5 DOFs). In that case, one could modify equation (4) to include bodies and true bars, but it is conceptually simpler to appreciate that some of the DOFs predicted by the CGK rule in 3D are simply bars rotating on their axes. Table 3 shows this effect. The simple cubic framework has 6 actual DOFs as predicted by the Maxwell rule; the CGK obtains 18 DOFs, 12 corresponding to the edges rotating on themselves, in addition to the 6 structural ones. The same arithmetic applies to the second framework: it is locked with no DOF, but the CGK rule proposes 18 DOFs, one for each bars (12 edges, 6 cross-linkers).

Table 3. Examples of counting rules for simple 3D frameworks

Framework	Maxwell	CGK
	$m - s = 3j - b - 6$	$m - s = 6(n - 1) - 6g + \sum_{i=1}^g f_i$
	(8, 12) $\Rightarrow m - s = 6$	(12, 16, 16 × 3) $\Rightarrow m - s = 18$
	(8, 18) $\Rightarrow m - s = 0$	(18, 28, 28 × 3) $\Rightarrow m - s = 18$

To conclude this comparison of the various counting schemes, we consider replacing the nodes of a graph by bodies in the CGK scheme. This is certainly relevant to MOFs as SBUs can be large. This procedure also greatly simplifies the counting of the number of joints g . But as can be seen in Table 2, this procedure adds DOFs, those related to the motion of the body-nodes. Some amount of un-resisted deformation (also compatible with a periodic network) follows from the rotation of the body-nodes as can be seen in fig. 3. On the other hand, due to steric effects, the amplitude of such modes is likely to be limited in real chemical frameworks.

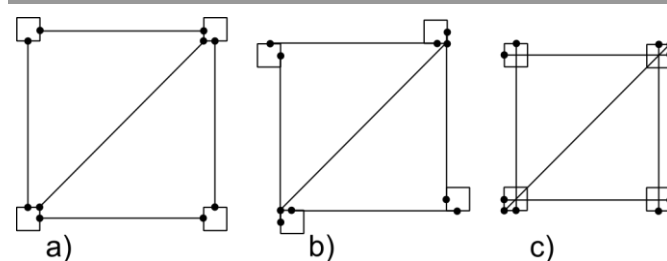


Fig. 3. Mode of deformation for a framework with body-nodes. From a) to c), the body-nodes are rotating counter-clockwise.

3.3 Scalar counting rules for periodic systems

The counting rules presented in sections 3.1 and 3.2 have been extended to the case of periodic frameworks³¹. The Maxwell rules transform into

$$(2D) \quad m - s = f + 4 = 2j - b + 1, \quad (5)$$

$$(3D) \quad m - s = f + 9 = 3j - b + 3. \quad (6)$$

The CGK rules become

$$(2D) \quad m - s = f + 4 = 3n + 1 - 3g + \sum_{i=1}^g f_i, \quad (7)$$

$$(3D) \quad m - s = f + 9 = 6n + 3 - 6g + \sum_{i=1}^g f_i. \quad (8)$$

On one hand, with reference to the non-periodic system, the corresponding periodic system gains additional DOFs; these derive simply from the unit cell (or unit vectors), with four extra DOFs in 2D and nine in 3D. On the other hand, the periodic systems lose DOFs from the fact that the freedom giving elements (joints j or bodies n) that are now periodic images are not counted; in a similar manner, extra DOFs are gained from constraints elements (bars b or joints g) being less

numerous in the unit cells. The net effects are illustrated in table 4 and 5. The bar-and-joint frameworks have the same number of DOFs than their non-periodic counterparts, but the body-and-joint frameworks have less. In general, periodic systems have less DOFs than corresponding non-periodic.

Table 4. Examples of counting rules for periodic 2D frameworks

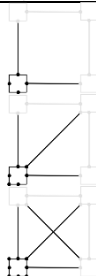
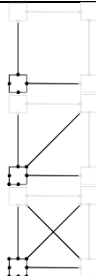
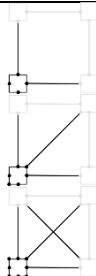
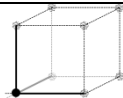
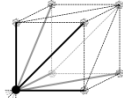
Framework	Periodic Maxwell $m - s = 2j - b + 1$	Periodic CGK $m - s = 3n + 1 - 3g + \sum_{i=1}^g f_i$
	$(\underline{1}, 2) \Rightarrow m - s = 1$	$(2, \underline{3}, 3 \times 1) \Rightarrow m - s = 1$
	$(\underline{1}, 3) \Rightarrow m - s = 0$	$(5, \underline{5}, 5 \times 1) \Rightarrow m - s = 0$
	$(\underline{1}, 4) \Rightarrow m - s = -1$	$(6, \underline{7}, 7 \times 1) \Rightarrow m - s = -1$
	N/A	$(3, \underline{4}, 4 \times 1) \Rightarrow m - s = 2$
	N/A	$(4, \underline{6}, 6 \times 1) \Rightarrow m - s = 1$
	N/A	$(5, \underline{8}, 8 \times 1) \Rightarrow m - s = 0$

Table 5. Examples of counting rules for periodic 3D frameworks

Framework	Periodic Maxwell $m - s = 3j - b + 3$	Periodic CGK $m - s = 6n + 3 - 6g + \sum_{i=1}^g f_i$
	$(\underline{1}, 3) \Rightarrow m - s = 3$	$(3, \underline{5}, 5 \times 3) \Rightarrow m - s = 6$
	$(\underline{1}, 6) \Rightarrow m - s = 0$	$(6, \underline{11}, 11 \times 3) \Rightarrow m - s = 6$

3.4 Application of scalar rules to 3D MOFs

In order to test the counting rules it is enough to limit the study to two frameworks, one flexible and one rigid.

The flexible system we have chosen is based on an augmented body centred cubic **pcb** net (equivalent to **bcu-a**). Fig. 4 displays the motif for a unit cell. Note that the choice of the hinges direction breaks the cubic symmetry. The elastic tensor for instance would have a tetragonal symmetry. This non-periodic assembly is a simplification of the periodic framework and comprises 2 SBUs, 8 bar bodies for the ligands, and 12 hinges. It is immediately apparent by visual inspection that a mechanism exists. The periodic version would be composed of 2 SBU bodies, 8 bar bodies and 16 hinges, again with at least one obvious mechanism. However, the non-periodic counting rules predicts $m - s = 6 \times 9 - 6 \times 12 + 12 \times 1 = -6$ and the

periodic one $m - s = 6 \times 10 + 3 - 6 \times 16 + 16 \times 1 = -17$. This is very disappointing, and shows not only that this assembly is heavily over-constrained, but that the number of states of self-stress conceals the mechanism we know to exist.

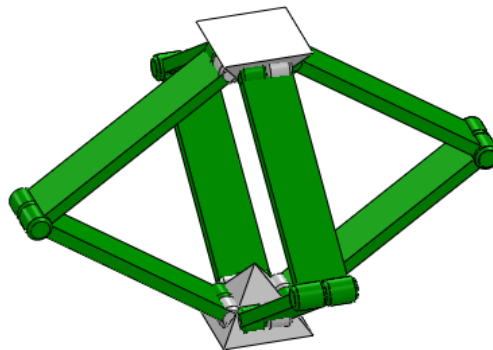


Fig. 4. Non-periodic model for a **pcb** framework.

The rigid system is based on the archetypical IRMOF-1 family, and models are depicted in Fig.5. It belongs to the **pcu-a** net, but with the added complexity that the hinges are oriented perpendicularly across the SBUs, leading to two possible cages, referred to as large pore or small pore, and to a sizeable unit cell consisting of eight cages. Following the example of ¹⁰, we start by considering a cage in isolation: both types are composed of 8 body-nodes, 12 body-bars and 24 hinges. IRMOF-1 is known to be rigid from several sources^{10, 37}, and the scalar counting rule for a non-periodic unit predicts $m - s = 6 \times 19 - 6 \times 24 + 24 \times 1 = -6$.

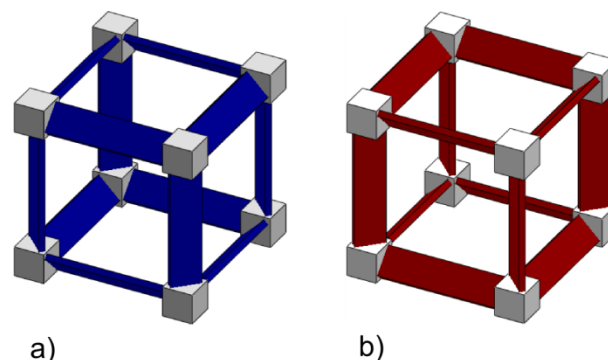


Fig. 5. Partial models for IRMOF-1 (**pcu-a** net): a) large pore, b) small pore. The light grey squares represent the SBUs and the dark grey plates represent the ligands. The ligands are linked to the SBUs by hinges (not drawn). The actual unit cell of IRMOF-1 contains alternating small and large pores cages, eight in total.

IRMOF-1 is correctly predicted to be rigid, but **pcb** is incorrectly predicted to be rigid. A counter-example is enough to conclusively prove that the scalar counting rules do not work for 3D MOFs. This was perhaps predictable, and a review of counting rules for robotic systems (non-periodic) reaches the same conclusion⁸. However, these simple scalar rules have allowed us to expose the basic concepts with basic arithmetic. Fortunately, it is possible to make use of symmetry to improve them significantly.

4 Group theoretical counting rules

4.1 Method

Several symmetry extended versions of the counting rules have been developed by Fowler and Guest, for bar-and-joint frameworks³⁸, for body-and-joint systems²⁸, with and without taking periodicity into account³¹. From the previous section on scalar rules, we have seen that in order to treat the joints between carboxylate linkers and SBUs correctly as chiefly hinge-like, a body-and-joint description is necessary. For periodic MOFs, it would be more generic to account for periodicity, but as we are introducing the method, we start with the non-periodic body-and-joint extension. This takes the form of equation (9)

$$\Gamma(m) - \Gamma(s) = (\Gamma(v, C) - \Gamma_{\parallel}(e, C) - \Gamma_0) \times (\Gamma_T + \Gamma_R) + \Gamma_f. \quad (9)$$

The different terms are discussed in detail in the following paragraphs, but this equation is similar to equation (4), the difference being that instead of just the number of mechanisms minus states of self-stress, it produces a group theoretical representation of the same. Therefore, if some states of self-stress belong to different irreducible representations (irrep) than the mechanisms, they will not cancel out. For instance, the resulting representation for our **pcb** test case is given by

$$\Gamma(m) - \Gamma(s) = A_{1g} - A_{2g} - B_{2g} - E_g - A_{1u} - 2B_{1u}. \quad (10)$$

The positive irreps, here A_{1g} alone, indicate the existence of mechanisms, while the negative irreps indicate self-stresses. It is important to note that some mechanisms and self-stresses might have the same symmetry and still cancel out, but with several irreps this is less likely.

But in order to obtain such a useful representation, it is necessary to resolve equation (9) first.

The first step consists in generating what Fowler and Guest call the contact polyhedron (C). This 3D graph has vertices (v) that correspond to the bodies of the system, and edges (e) that correspond to the joints (hinges for carboxylate MOFs). C is not always an actual polyhedron and is certainly not unique (for a detailed discussion, see³⁹), but it is generally straightforward to produce one. Figures 6 and 7 display the contact polyhedra for **pcb** and simplified IRMOF-1 cages.

At the second step, the point group $G(C)$ of the contact polyhedron that also respects the axes of the hinges is determined. This is why it is actually useful to decorate C with segment representing such axes at the first stage.

The third step is very simple: the representation $\Gamma_T + \Gamma_R$ is read from the character table⁴⁰ of $G(C)$. For several symmetries (at least all improper ones), its character is zero, which is important to note in order to avoid unnecessary labour for some other representations.

For the fourth step, the characters for the remaining representations in the first term of (9) are determined by inspection on C . For a given symmetry operation, the character of $\Gamma(v, C)$ is the number of nodes (points) of C that are unshifted and the character of $\Gamma_{\parallel}(e, C)$ is the number of vectors along the edges of C

that are unshifted minus the number of vectors that are inverted on their edge. Γ_0 is the trivial representation with a character of 1 for all symmetries. Only the characters for columns where the character from $\Gamma_T + \Gamma_R$ differs from zero have to be calculated, as the resulting product will be null anyway.

The fifth step is the most difficult, conceptually, and because it does not benefit from the zeroes of $\Gamma_T + \Gamma_R$. For MOFs with hinges perpendicular to the ligand, the characters of the representation of the freedoms Γ_f can be obtained from the fact that for each symmetry operation, the character of the hinge χ_{hinge} is the product of the character χ_R of a rotation (axial vector, pseudovector) on the hinge axis by the character $\chi_{\parallel e}$ of a (radial) vector on the edge e . Alternately the table in Figure 4 from²⁸ can be used.

Finally, the various additions, subtractions and multiplications can be applied to the representations to obtain $\Gamma(m) - \Gamma(s)$, which can then be projected onto the irreps. We used spreadsheets developed by Niece⁴¹ to speed up these routine tasks. The electronic supplementary information contains a step-by-step derivation for the **pcb** assembly.

4.2 Face centred cubic MOF with **pcb** net

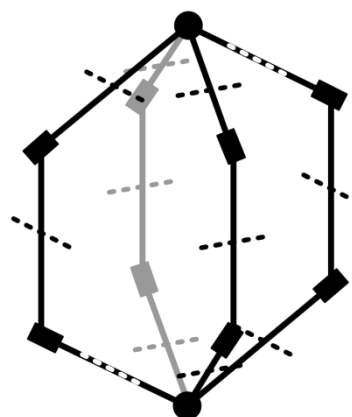


Fig. 6. Contact polyhedron for the **pcb** assembly. The vertices represent the two types of bodies, discs for SBU, rectangle for ligands (still simply treated as points for symmetry operations). The solid lines are the edges of the polyhedron and represent the hinges. They are decorated by segment in dashed line indicating the axis of the hinges. This polyhedron belongs to the D_{4h} point group

The calculations for the **pcb** assembly are shown in tabular form in table 6.

Table 6. Calculations for the **pcb** assembly

D_{4h}	E	$2C_4$	C_2	$2C_2'$	$2C_2''$	i	$2S_4$	σ_h	$2\sigma_v$	$2\sigma_d$
$\Gamma(v, C)$	10	2	2	0	0	-	-	-	-	-
$\Gamma_{ }(e, C)$	12	0	0	-2	0	-	-	-	-	-
Γ_0	1	1	1	1	1	-	-	-	-	-
=	-3	1	1	1	-1	-	-	-	-	-
\times										
$\Gamma_T + \Gamma_R$	6	2	-2	-2	-2	0	0	0	0	0
=	-18	2	-2	-2	2	0	0	0	0	0
$+$										
Γ_f	12	0	0	2	0	0	0	4	6	0
= $\Gamma(m)$										
$-\Gamma(s)$	-6	2	-2	0	2	0	0	4	6	0
$\Gamma(m) - \Gamma(s) = [A_{1g}] - A_{2g} - B_{2g} - E_g - A_{1u} - 2B_{1u}$										

The character of the identity E is equal to -6 , which is the same result as the scalar counting rules. $\Gamma(m) - \Gamma(s)$ contains one non degenerate positive irrep. The negative terms contribute -7 . The mechanism with irrep A_{1g} is revealed by this analysis, as the states of self-stress do not conceal it in the higher dimension symmetry space. This is only one example, but it already shows a great improvement over the scalar rule.

4.2 IRMOF-1

In order to have confidence in the predictive power of the group theoretical counting rules, they should also be able to correctly characterise a rigid system.

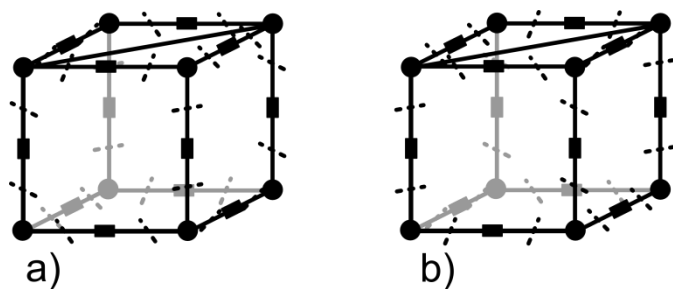


Fig. 7. Contact polyhedra for IRMOF-1 cages, a) large pore, b) small pore. The vertices represent the two types of bodies, circles for SBU, rectangle for ligands (still simply treated as points for symmetry operations). The solid lines are the edges of the polyhedron and represent the hinges. They are decorated by segment in dashed line indicating the axis of the hinges. Both polyhedra belong to the O_h point group

The calculations for both large and small pore models are given in table 7 and 8.

Table 7. Calculations for IRMOF-1, large pores

O_h	E	$8C_3$	$6C_2$	$6C_4$	$3C_2$	i	$6S_4$	$8S_6$	$3\sigma_h$	$6\sigma_d$
$\Gamma(v, C)$	20	-	2	0	0	-	-	-	-	-
$\Gamma_{ }(e, C)$	24	-	0	0	0	-	-	-	-	-
Γ_0	1	-	1	1	1	-	-	-	-	-
=	-5	-	1	-1	-1	-	-	-	-	-
\times										
$\Gamma_T + \Gamma_R$	6	0	-2	2	-2	0	0	0	0	0
=	-30	0	-2	-2	2	0	0	0	0	0
$+$										
Γ_f	24	0	0	2	0	0	0	0	0	4
= $\Gamma(m)$										
$-\Gamma(s)$	-6	0	-2	-2	2	0	0	0	0	4
$\Gamma(m) - \Gamma(s) = -T_{1g} - A_{1u} + [A_{2u}] - T_{2u}$										

Surprisingly, the analysis for the large pore cage seems to reveal a mechanism. At first, this appears contrary to the results from the mechanical model of an IRMOF-1 cage¹⁰. Careful reading shows that this mechanical model was in fact of a small pore cage. Is it really possible that the large pore cage is flexible while the small pore care is rigid?

Table 8. Calculations for IRMOF-1, small pores

O_h	E	$8C_3$	$6C_2$	$6C_4$	$3C_2$	i	$6S_4$	$8S_6$	$3\sigma_h$	$6\sigma_d$
$\Gamma(v, C)$	20	-	2	0	0	-	-	-	-	-
$\Gamma_{ }(e, C)$	24	-	0	0	0	-	-	-	-	-
Γ_0	1	-	1	1	1	-	-	-	-	-
=	-5	-	1	-1	-1	-	-	-	-	-
\times										
$\Gamma_T + \Gamma_R$	6	0	-2	2	-2	0	0	0	0	0
=	-30	0	-2	-2	2	0	0	0	0	0
$+$										
Γ_f	24	0	0	2	0	0	0	0	0	-4
= $\Gamma(m)$										
$-\Gamma(s)$	-6	0	-2	-2	2	0	0	0	0	-4
$\Gamma(m) - \Gamma(s) = -A_{1g} + [A_{2g}] - T_{2g} - T_{1u}$										

No, not really: the analysis for the small pore cage also reveals a mechanism, albeit one with a different irrep.

Figure 8 shows the two deformation modes. They have different characters, a rhombohedral distortion for the large pore cage, and a twisting mechanism for the small pore cage. The authors of ¹⁰ were somewhat unfortunate to choose the small pore cage, as the corresponding twisting mechanism is much less apparent than the rhombohedral distortion of the large pore cage.

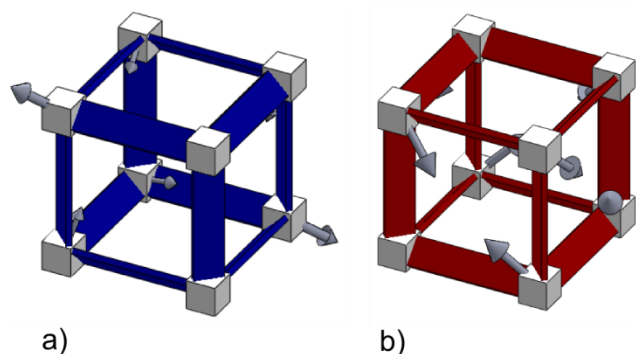


Fig. 8. Deformation of the two IRMOF-1 cages, a) large pore, b) small pore.

When arrayed in the periodic network of IRMOF-1, the two deformations are not compatible, and the larger cell is not flexible. This is confirmed by carrying the group theoretical analysis for the full unit cell of IRMOF-1, as shown in table 9. The contact polyhedron C is large, and is not pictured, but it belongs to the tetrahedral group T_d .

Table 9. Calculations for IRMOF-1, full unit cell

T_d	E	$8C_3$	$3C_2$	i	$6S_4$	$6\sigma_d$
$\Gamma(v, C)$	81	-	5	-	-	-
$\Gamma_{\parallel}(e, C)$	108	-	4	-	-	-
Γ_0	1	-	1	-	-	-
$=$	-28	-	0	-	-	-
\times						
$\Gamma_T + \Gamma_R$	6	0	-2	0	0	0
$=$	-168	0	0	0	0	0
$+$						
Γ_f	108	0	-4	0	0	0
$= \Gamma(m)$						
$-\Gamma(s)$	-60	0	-4	0	0	0
$\Gamma(m) - \Gamma(s) = -3A_1 - 3A_2 - 6E - 7T_1 - 7T_2$						

For the full unit cell, there are no mechanisms, all the contributions to $\Gamma(m) - \Gamma(s)$ are states of self-stress.

These are just examples, and do not prove that the group theoretical counting rules can be applied successfully to all MOFs. They show great promise however and have already helped correct a minor misunderstanding on the causes of the rigidity of IRMOF-1.

5 Conclusion

This preliminary study has obtained two main results.

Firstly, scalar counting rules definitely cannot establish the flexibility/rigidity of periodic MOF networks nor even of simplified MOF-like non-periodic assemblies.

Secondly, symmetry extended group theoretical counting rules seem to be able to correct these shortcomings and predict flexibility/rigidity, and this without a huge cost in complexity, nor computational power required.

While this method is very promising, additional work is needed to cement its use. For a start, the periodic extension³¹ of equation (9) should be used to calculate the representation of

mechanisms and /or states of self-stress of MOFs. Fortunately, the procedure is very similar to the one highlighted in this work for isolated structures.

This fully periodic analysis should then be applied to many more nets to confirm predictive power. Such a high-throughput approach would certainly benefit from automation (if only to reduce the risk of errors), but this highlights a difficulty with the method: it is still essentially a pen and paper affair, but implementing it in software form would require a significant effort.

In our examples, we are limiting the analysis to the presence or not of mechanisms. More information can be obtained from symmetry, for instance it should be possible to determine whether a mechanism is finite (as opposed to infinitesimal)⁴².

Conversely, symmetry alone is generally not enough to determine the deformation mode, in the same way that it is not enough to obtain the vibration modes of molecules and phonons of crystals⁴⁰.

Another limitation of the method is that it treats ligands and SBUs as mechanical objects that only interact through joints. Other interactions, such as π - π orbitals overlaps or hydrogen-bonds are not considered and it is unlikely that the formalism can even handle them.

Finally, the building blocks, SBU and ligands, are not rigid mechanical bodies, but deformable chemical entities. The method can only be meaningful if the joints between SBUs and ligands are significantly more compliant than the SBUs and ligands themselves. If the symmetry of the system prohibits flexibility of the framework, the deformations of ligands and/or of the SBUs are likely to become more relevant for the compliance or low-energy vibrations of the rigid MOFs as was shown by Rimmer and co-workers for IRMOF-1⁴³. It might be possible in principle to break down the mechanical ligands and SBUS into sub-units and carry out a group-theoretical analysis, but we reckon it would be mostly meaningless in the absence of information on the relative stiffness of the joints.

But all considered, group theoretical counting rules provide an elegant, relatively simple and cheap method of establishing whether the underlying framework of a MOF can sustain mechanisms of flexibility.

Acknowledgements

This work was supported by the Engineering and Physical Sciences Research Council [Grant number EP/G064601/1].

ASHM would like to thank Ash Marmier for the provision of toy cubes used in the manufacture of mechanical models of MOFs.

Notes and references

^a College of Engineering, Mathematics and Physical Science, University of Exeter, EX4 4QF, UK.

[†] Electronic Supplementary Information (ESI) available: step-by-step derivation for the **pcb** assembly and group theoretical calculations in spreadsheet form See DOI: 10.1039/c000000x/

[‡] Corresponding author: a.s.h.marmier@exeter.ac.uk

1. P. Horcajada, R. Gref, T. Baati, P. K. Allan, G. Maurin, P. Couvreur, G. Ferey, R. E. Morris and C. Serre, *Chem. Rev.*, 2012, **112**, 1232-1268.
2. C. E. Wilmer, M. Leaf, C. Y. Lee, O. K. Farha, B. G. Hauser, J. T. Hupp and R. Q. Snurr, *Nature Chemistry*, 2012, **4**, 83-89.
3. C. E. Wilmer, O. K. Farha, Y.-S. Bae, J. T. Hupp and R. Q. Snurr, *Energy & Environmental Science*, 2012, **5**, 9849-9856.
4. C. S. Borcea and I. Streinu, *Proceedings of the Royal Society a-Mathematical Physical and Engineering Sciences*, 2010, **466**, 2633-2649.
5. C. Borcea, I. Streinu and S. Tanigawa, *SIAM Journal on Discrete Mathematics*, 2015, **29**, 93-112.
6. S. C. Power, *New York Journal of Mathematics*, 2014, **20**, 665-693.
7. C. Calladine, *International Journal of Solids and Structures*, 1978, **14**, 161-172.
8. G. Gogu, *Mechanism and Machine Theory*, 2005, **40**, 1068-1097.
9. A. Sartbaeva, S. A. Wells, M. M. J. Treacy and M. F. Thorpe, *Nature Materials*, 2006, **5**, 962-965.
10. L. Sarkisov, R. L. Martin, M. Haranczyk and B. Smit, *J. Am. Chem. Soc.*, 2014, **136**, 2228-2231.
11. K. D. Hammonds, V. Heine and M. T. Dove, *J. Phys. Chem. B*, 1998, **102**, 1759-1767.
12. X. Kong and C. M. Gosselin, in *Advances in robot kinematics*, Springer, 2002, pp. 453-462.
13. L. Pauling, *Zeitschrift Fur Kristallographie*, 1930, **74**, 213-225.
14. M. T. Dove, V. Heine and K. D. Hammonds, *Mineralogical Magazine*, 1995, **59**, 629-639.
15. M. F. Thorpe and Y. Cai, *J. Non-Cryst. Solids*, 1989, **114**, 19-24.
16. V. Kapko, C. Dawson, M. M. J. Treacy and M. F. Thorpe, *PCCP*, 2010, **12**, 8531-8541.
17. C. J. Dawson, V. Kapko, M. F. Thorpe, M. D. Foster and M. M. J. Treacy, *Journal of Physical Chemistry C*, 2012, **116**, 16175-16181.
18. A. L. Goodwin and C. J. Kepert, *Physical Review B*, 2005, **71**, 140301.
19. A. L. Goodwin, *Physical Review B*, 2006, **74**, 134302.
20. S. A. Wells and A. Sartbaeva, *Molecular Simulation*, 2015, 1-13.
21. G. Ferey and C. Serre, *Chem. Soc. Rev.*, 2009, **38**, 1380-1399.
22. A. U. Ortiz, A. Boutin, A. H. Fuchs and F.-X. Coudert, *Phys. Rev. Lett.*, 2012, **109**.
23. A. U. Ortiz, A. Boutin, A. H. Fuchs and F. X. Coudert, *J. Chem. Phys.*, 2013, **138**, 174703.
24. A. U. Ortiz, A. Boutin and F. X. Coudert, *Chem. Commun.*, 2014, **50**, 5867-5870.
25. S. Pellegrino and C. R. Calladine, *International Journal of Solids and Structures*, 1986, **22**, 409-428.
26. S. D. Guest and J. W. Hutchinson, *J. Mech. Phys. Solids*, 2003, **51**, 383-391, Pii s0022-5096(02)00107-2.
27. V. Kapko, C. Dawson, I. Rivin and M. M. J. Treacy, *Phys. Rev. Lett.*, 2011, **107**, 164304.
28. S. D. Guest and P. W. Fowler, *Mechanism and Machine Theory*, 2005, **40**, 1002-1014.
29. P. W. Fowler, S. D. Guest and T. Tarnai, *Symmetry*, 2014, **6**, 368-382.
30. P. W. Fowler and S. D. Guest, *Proceedings of the Royal Society a-Mathematical Physical and Engineering Sciences*, 2005, **461**, 1829-1846.
31. S. D. Guest and P. W. Fowler, *Philosophical Transactions of the Royal Society a-Mathematical Physical and Engineering Sciences*, 2014, **372**, 20120029.
32. M. O'Keeffe, M. A. Peskov, S. J. Ramsden and O. M. Yaghi, *Acc. Chem. Res.*, 2008, **41**, 1782-1789.
33. J. C. Maxwell, *The London, Edinburgh, and Dublin Philosophical Magazine and Journal of Science*, 1864, **27**, 294-299.
34. P. A. Tchebychev, *Théorie des mécanismes connus sous le nom de parallélogrammes*, Imprimerie de l'Académie impériale des sciences, 1853.
35. M. Grübler, *Eine Theorie des Zwanglaufes und der ebenen Mechanismen*. Verlag von Julius Springer, Berlin, 1917.
36. K. Kutzbach, *Maschinenbau*, 1929, **8**, 710-716.
37. D. F. Bahr, J. A. Reid, W. M. Mook, C. A. Bauer, R. Stumpf, A. J. Skulan, N. R. Moody, B. A. Simmons, M. M. Shindel and M. D. Allendorf, *Physical Review B*, 2007, **76**, 184106.
38. P. W. Fowler and S. D. Guest, *International Journal of Solids and Structures*, 2000, **37**, 1793-1804.
39. B. Schulze, S. D. Guest and P. W. Fowler, *International Journal of Solids and Structures*, 2014, **51**, 2157-2166.
40. F. A. Cotton, *Chemical applications of group theory*, John Wiley & Sons, 2008.
41. B. K. Niece, *J. Chem. Educ.*, 2012, **89**, 1604-1605.
42. S. D. Guest and P. W. Fowler, *Journal of Mechanics of Materials and Structures*, 2007, **2**, 293-301.
43. L. H. Rimmer, M. T. Dove, A. L. Goodwin and D. C. Palmer, *PCCP*, 2014, **16**, 21144-21152.